

# Thermal regimes of high burn-up nuclear fuel rod

Nikolai A. Kudryashov, Aleksandr V. Khlunov,  
Mikhail A. Chmykhov

Department of Applied Mathematics, National Research  
Nuclear University MEPhi, 31 Kashirskoe Shosse, 115409  
Moscow, Russian Federation

## Abstract

The temperature distribution in the nuclear fuel rods for high burn-up is studied. We use the numerical and analytical approaches. It is shown that the time taken to have the stationary thermal regime of nuclear fuel rod is less than one minute. We can make the inference that the behavior of the nuclear fuel rod can be considered as a stationary task. Exact solutions of the temperature distribution in the fuel rods in the stationary case are found. Thermal regimes of high burn-up the nuclear fuel rods are analyzed.

## 1 Introduction

Temperature distribution in the fuel rod of nuclear reactor is one of the most important factors that controls the behavior of fission products in the pellets, the diffusion and vaporization properties and so on [1]. This dependence has been intensively studied for prolonged lifetime of existing reactors. There are many papers in which the authors studied the different aspects of this problem [2–7]. Yapici et al. [2] investigated the maximum temperatures in centerline of the fuel rod for different clad outer surface temperatures, melting points of the fuel materials, temporal heat generation, temperature distribution in the nuclear fuel rod and temporal variation of the neutronic data during rejuvenation periods. In [3] Kim et al. developed the one-dimensional heat conduction model to determine the temperatures distribution from the fuel center to cladding surface in the radial direction.

Pontedeiro et al. in [4] presented an improved lumped—differential formulation for one—dimensional transient heat conduction in a heat generating cylinder with temperature—dependent thermo—physical properties typical of high burn-up nuclear fuel rods. Analytical model for the determination of the temperature distribution in cylindric heater components with characteristics of nuclear fuel rods is given by Fortini et al. in [5]. Espinosa—Paredas et al. in paper [7] explored the applicability of a fuel rod mathematical model based on Non—Fourier transient heat conduction as constitutive law for the Light Water Reactors transient analysis.

The fuel behavior is affected by the temperature distribution in the fuel that is related to change in the fuel microstructure with irradiation [18]. One significant change in the fuel microstructure is the formation of a porous rim in the periphery of the high burn-up fuel [8–17]. High burn-up nuclear fuel rods have been intensively studied last years [4]. Many papers were published studying of the rim formation mechanism [18–20]. It was shown that the rim structure is formed through recrystallization and coarsened pore formation. The subdivided grains with high angle grain boundaries are the nuclei of recrystallization, and then the coarsened pores are formed by the sweeping out of small pores during grain growth on recrystallization [18–20]. The rim structure can be described taking into consideration many specific characteristics of the fuel [18] but in this paper we are not going to touch these interesting questions.

Here we study the temperature distribution in the nuclear fuel rod of the reactor taking the influence of the high burn-up into account. Using the numerical method based on the difference equation of the heat conductivity we prove that the stationary behavior of the nuclear reactor is reached for the time less then one minute. This fact allows us to consider the temperature distribution using the stationary cases of the heat conductivity in the nuclear fuel reactor. At solution of the task we do not use the modern approaches for the nonintegrable differential equations (see [21–23]). The task is solved by us taking the simple integration of equations. As a result we find the solution for the temperature distribution in the nuclear fuel rod in the analytical form for the stationary behavior of the reactor. Exact solutions allow us to analyze the temperature distribution in details and to evaluate the influence of the rim - layer and the zirconium oxide on the temperature distribution in the nuclear fuel rod.

This paper is organized as follows. In section 2 we present the statement of the problem and we use the numerical methods to obtain the energy flow on the surface of cladding. Using the numerical simulation for solving task in section 3 we observe that the stationary case of the temperature distribution in the nuclear fuel rod arises very quickly in comparison with time of the

product of electricity production. So we can consider the stationary temperature distribution in the nuclear fuel rod. Using this fact in section 4 we give the stationary statement of the problem and in section 5 we find the exact solution of the temperature distribution in the nuclear fuel rod taking rim - layer and zirconium oxide into account for high burn-up fuel. In section 6 we discuss the particularities of the stationary thermal regimes in nuclear rods. As this takes place we consider the different cases of nuclear fuel rods: with gap and without gap; in the case of the burn-up and without rim - layer and zirconium and so on. We can allow to do it using the analytical solutions.

## 2 The statement of the problem for the temperature distribution in nuclear fuel rod with rim — layer and zirconium oxide

The geometry of the nuclear fuel rod is given in Fig. 1. We take this geometry into account in this paper to study the temperature distribution in the nuclear fuel rod.

Let us introduce the following notation:  $T_1(r, t)$  is dependence of temperature on  $r$  and  $t$  in the fuel that is  $UO_2$ ,  $T_2(r, t)$  is the dependence of temperature from radius and time in the gap, that is  $He$ ,  $T_3(r, t)$  is dependence of temperature on  $r$  and  $t$  in the cladding,  $\tilde{T}_1(r, t)$  is temperature in the rim layer,  $\tilde{T}_3(r, t)$  is the temperature in the zirconium oxide,  $r_0$  is the radius of the central hole,  $R_0$  is the radius of the nuclear fuel,  $R_1$  is the external radius of the gap in the fuel rod,  $R_2$  is the radius of the cladding,  $\tilde{R}_0$  is the internal radius of the rim - layer,  $\tilde{R}_2$  is the external radius of the zirconium oxide.

Nonlinear differential equation for the description of the temperature in the nuclear fuel rod can be written as

$$C_p(r, T) \rho(r, T) \frac{\partial T}{\partial t} = \frac{1}{r} \frac{\partial}{\partial r} \left( \lambda(r, T) r \frac{\partial T}{\partial r} \right) + q(r), \quad r_0 \leq r \leq R_2, \quad (1)$$

where  $C_p(r, T)$  is the specific heat capacity,  $\rho(r, T)$  is the mass density,  $\lambda(r, T)$  is the thermal conductivity,  $q(t)$  is the uniform volumetric heat generation rate which is independent of the temperature.

We take the initial condition for the temperature in the form

$$T(r, t = 0) = \varphi_0. \quad (2)$$

We used different initial conditions for the numerical simulation taking into account the initial behavior of nuclear reactor.

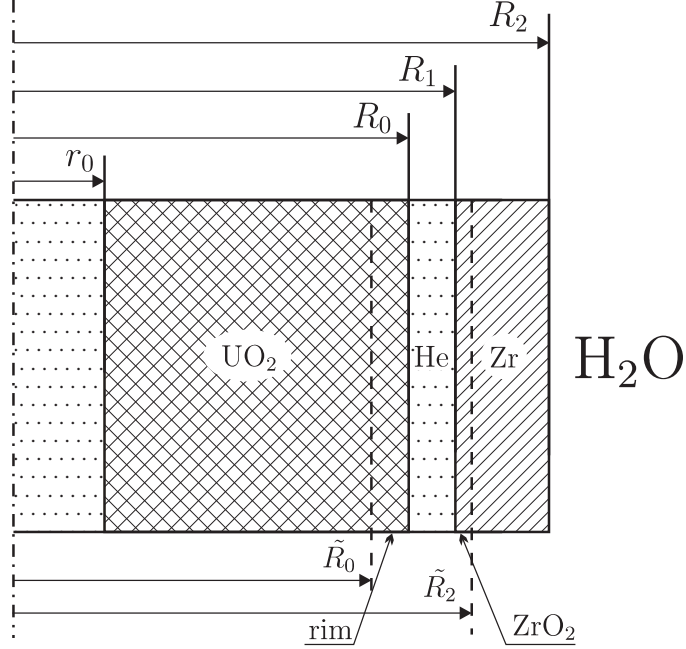


Figure 1: Geometry of the nuclear fuel rod:  $r_0$  is central hole,  $R_0$  is radius of the fuel,  $\tilde{R}_0$  is the radius of the rim layer,  $R_1$  is external radius of gap,  $\tilde{R}_2$  is radius of  $ZrO_2$ ,  $R_2$  is external radius of  $Zr$ .

The boundary values for the numerical simulation we took at  $r = r_0$  in the form

$$\left. \frac{\partial T}{\partial r} \right|_{r=r_0} = 0, \quad (3)$$

and at  $r = R_2$

$$T(r = R_2, t) = T_w, \quad (4)$$

where  $T_w$  is the temperature of the wall.

Heat capacity ( $C_p$ ) of oxide fuels is very important parameter for evaluation of fuel temperature at normal, transient and accidental conditions of light water reactor [1]. Heat capacities of undoped and impurity-doped  $UO_2$  pellets have been measured by many researchers. The values for densities and heat capacities of nuclear fuel, rim layer, gas in gap and in cladding are different from each other. We take formulae for these values as sectionally -

continuous function

$$\rho(r, T) C_p(r, T) = \begin{cases} \rho_1(T) C_{p,1}(T), & \text{if } r_0 \leq r < \tilde{R}_0, \\ \tilde{\rho}_1(T) \tilde{C}_{p,1}(T), & \text{if } \tilde{R}_0 \leq r < R_0, \\ \rho_2 C_{p,2}, & \text{if } R_0 \leq r < R_1, \\ \tilde{\rho}_3 \tilde{C}_{p,3}, & \text{if } R_1 \leq r < \tilde{R}_2, \\ \rho_3 C_{p,3}, & \text{if } \tilde{R}_2 \leq r < R_2. \end{cases}$$

We have taken physical parameters and dependencies of the densities and the specific heat capacities on temperature for the fuel, the gap and the cladding from the papers [1, 6, 7] .

Heat conductivities for the fuel and for the rim layer could be expressed by a classical phonon transport model [24–27]

$$\lambda_1(T) = \frac{1}{A + cbu + BT}, \quad (5)$$

where  $A$ ,  $B$  and  $c$  are constants and  $bu$  is the local burn-up in the nuclear fuel and in the rim - layer.

For numerical simulation of the temperature distribution in the nuclear fuel and in the rim - layer We assume that the coefficient of the heat conductivity is expressed by the sectionally - continuous function

$$\lambda(T, r) = \begin{cases} \frac{1}{A+BT}, & \text{if } r_0 \leq r < \tilde{R}_0 \\ \frac{1}{A_1+B_1T}, & \text{if } \tilde{R}_0 \leq r < R_0 \\ \lambda_1, & \text{if } R_0 \leq r < R_1 \\ \tilde{\lambda}_2, & \text{if } R_1 \leq r < \tilde{R}_2 \\ \lambda_2, & \text{if } \tilde{R}_2 \leq r < R_2, \end{cases}$$

where  $A$ ,  $B$ ,  $A_1$ ,  $B_1$ ,  $\lambda_1$ ,  $\tilde{\lambda}_1$ ,  $\tilde{\lambda}_2$ ,  $\lambda_2$  are constants. For numerical simulation of task we have taken values of these parameters from papers [24–27].

The volumetric heat generation rate for the numerical simulation can be written as

$$q(r) = \begin{cases} q_0, & \text{if } r_0 \leq r < \tilde{R}_0 \\ q_1, & \text{if } \tilde{R}_0 \leq r < R_0 \\ 0, & \text{if } R_0 \leq r < R_2, \end{cases}$$

where  $q_0$  and  $q_1$  are constants. Task (1) - (4) is solved by us in the next section using the numerical methods.

### 3 The numerical simulation of the temperature distribution in the nuclear fuel rod

Consider the equation

$$C_p(r, T) \rho(r, T) \frac{\partial T}{\partial t} = \frac{1}{r} \frac{\partial}{\partial r} \left( \lambda(r, T) r \frac{\partial T}{\partial r} \right) + q(r), \quad r_0 \leq r \leq R_2, \quad (6)$$

Multiplying (6) on  $r$  and integrating with respect to  $r$  at constant  $q$  and  $q_1$ , we have

$$\frac{\partial E}{\partial t} = 2\pi \int_{r_0}^{R_2} r \lambda(r, T) \frac{\partial T}{\partial r} dr + \pi q (\tilde{R}_0^2 - r_0^2) + \pi q_1 (R_0^2 - \tilde{R}_0^2), \quad (7)$$

where

$$E = 2\pi \int_{r_0}^{R_2} C_p(r, T) \rho(r, T) T(r, t) dr$$

Let us denote the flow of energy via the surface unit as  $W$ , then Eq.(6) can be written as

$$\frac{\partial E}{\partial t} = -2\pi R_2^2 W + \pi q (\tilde{R}_0^2 - r_0^2) + \pi q_1 (R_0^2 - \tilde{R}_0^2), \quad (8)$$

We obtain that the flow of energy for stationary behavior of the nuclear fuel rod takes the form

$$W = \frac{1}{2R_2^2} \left( q (\tilde{R}_0^2 - r_0^2) + q_1 (R_0^2 - \tilde{R}_0^2) \right), \quad (9)$$

To solve the task (1) - (4) we use the numerical simulation. With this aim we introduce the grid on coordinate  $r$  and time  $t$ . We take points on  $r$  and  $t$  using the formulae

$$r_j = j h, \quad (j = 0, \dots, J); \quad t^n = \tau n, \quad (n = 0, \dots, N), \quad (10)$$

where  $h$  and  $\tau$  are steps on coordinate and time,  $J$  corresponds to the radius  $R_2$ ,  $N$  corresponds to the stationary state of the nuclear fuel rod.

Let us introduce the grid functions at  $t = t^n$  and  $r = r_j$ . In this case we have

$$T(r_j, t^n) \simeq T_j^n, \quad q_j^n \simeq q(r_j, t^n), \quad (11)$$

$$\lambda_j^n \simeq \lambda(T_j^n, r_j), \quad C_p(T_j^n, r_j) \simeq C_{p,j}^n, \quad \rho(T_j^n, r_j) \simeq \rho_j^n.$$

We change the differential operators in Eq.(1) on difference operators using the formulae

$$\frac{\partial T}{\partial t} \Big|_{r=hj; t=\tau n + \frac{\tau}{2}} \simeq \frac{T_j^{n+1} - T_j^n}{\tau}, \quad \frac{\partial T}{\partial r} \Big|_{r=hj + \frac{h}{2}; t=\tau(n+1)} \simeq \frac{T_{j+1}^{n+1} - T_j^{n+1}}{h}, \quad (12)$$

Taking the grid functions (11) and the approximation of differential relations (12) we have the following difference equation which is approximately equivalent to (1)

$$\begin{aligned} \frac{T_j^{n+1} - T_j^n}{\tau} &= \Lambda_{j+\frac{1}{2}}^n \sqrt{\frac{r_{j+1}}{r_j}} \left( \frac{T_{j+1}^{n+1} - T_j^{n+1}}{h^2} \right) - \\ &- \Lambda_{j-\frac{1}{2}}^n \sqrt{\frac{r_{j-1}}{r_j}} \left( \frac{T_j^{n+1} - T_{j-1}^{n+1}}{h^2} \right) + f_j^n, \quad f_j^n = \frac{q_j^n}{C_{p,j}^n \rho_j^n}, \end{aligned} \quad (13)$$

$$(j = 1, \dots, J-1),$$

where we use notation

$$\Lambda_{j+\frac{1}{2}}^n = \frac{\lambda_j^n + \lambda_{j+1}^n}{2 C_{p,j}^n \rho_j^n}, \quad \Lambda_{j-\frac{1}{2}}^n = \frac{\lambda_j^n + \lambda_{j-1}^n}{2 C_{p,j}^n \rho_j^n}, \quad (j = 1, \dots, J-1). \quad (14)$$

Difference equation (13) can be written as

$$A_j^n T_{j+1}^{n+1} - D_j^n T_j^{n+1} + B_j^n T_{j-1}^{n+1} = F_j^n, \quad (15)$$

where

$$A_j^n = \frac{\tau}{h^2} \sqrt{\frac{r_{j+1}}{r_j}} \left( \frac{\lambda_j^n + \lambda_{j+1}^n}{2 C_{p,j}^n \rho_j^n} \right), \quad (16)$$

$$D_j^n = 1 + \frac{\tau}{h^2} \sqrt{\frac{r_{j+1}}{r_j}} \left( \frac{\lambda_j^n + \lambda_{j+1}^n}{2 C_{p,j}^n \rho_j^n} \right) + \frac{\tau}{h^2} \sqrt{\frac{r_{j-1}}{r_j}} \left( \frac{\lambda_j^n + \lambda_{j-1}^n}{2 C_{p,j}^n \rho_j^n} \right), \quad (17)$$

$$B_j^n = \frac{\tau}{h^2} \sqrt{\frac{r_{j-1}}{r_j}} \left( \frac{\lambda_j^n + \lambda_{j-1}^n}{2 C_{p,j}^n \rho_j^n} \right), \quad (18)$$

$$F_j^n = -T_j^n - \tau f_j^n. \quad (19)$$

Difference equations (15) are the system of the algebraic equations which corresponds to the differential equation (1). This system of equations allows us to find the temperature distribution taking the boundary values and initial conditions.

We assume that the temperature distribution on time  $t^n = n\tau$  is known. The task is to solve the system of the algebraic equations and to find the temperature distribution at the moment  $t^{n+1} = (n+1)\tau$ .

From the initial condition we know that  $T(r, t = 0) = \varphi_0$  and consequently we know the temperature distribution on the radius at  $n = 0$

$$T_j^0 = \varphi_0 \quad (20)$$

Taking into consideration the boundary conditions (3) and (4), we have

$$T_1^n = T_0^n, \quad T_J^n = T_l, \quad (n = 0, \dots, N) \quad (21)$$

Using the temperature distribution on the first layer on time (20) and conditions (21), we solve the system of the algebraic equations (15) and find the temperature on the first layer at  $t^1 = \tau$ . Then taking into consideration values  $T_j^1$ , we obtain values of temperature  $T_j^2$  at  $t^2 = 2\tau$  and so on.

The system of algebraic equations (15) can be solved by the sweep method.

On figure 2 we can see the evolution on temperature in nuclear fuel rod in the case  $q_L = 200$  W/cm. Here and later  $q_L = q_0 \pi (\tilde{R}_0^2 - r_0^2) + q_1 \pi (R_0^2 - \tilde{R}_0^2)$ , where  $q_1 = 2q_0$ . We have used the initial condition for the temperature assuming that this temperature is equal to temperature of the wall

$$T(r, t = 0) = T_w \quad (22)$$

Other parameters of the mathematical model are used from the table 1.

From figure 2 we can see that the stationary state of the nuclear fuel rod with burn-up is reached during 30 second of time.

Figure 3 demonstrates the output the temperature to the stationary regime of the nuclear fuel rod at the different values of the volumetrical source rate. We can observe that the time of the output on the stationary state is not more then 30 seconds. Therefore the basic temperature regimes of the nuclear fuel rods are the stationary regimes and we can consider the temperature distribution in the nuclear fuel rod as the stationary task.

The numerical simulation of dependence for the heat flow on time at  $r = R_2$  is given on figure 4. From this figure we can see that the time from the initial state to the stationary behavior is 40 seconds. This time depends on the value of source and the time grows with increasing source. However this time is not more 45 seconds for available sources in nuclear fuel rod.



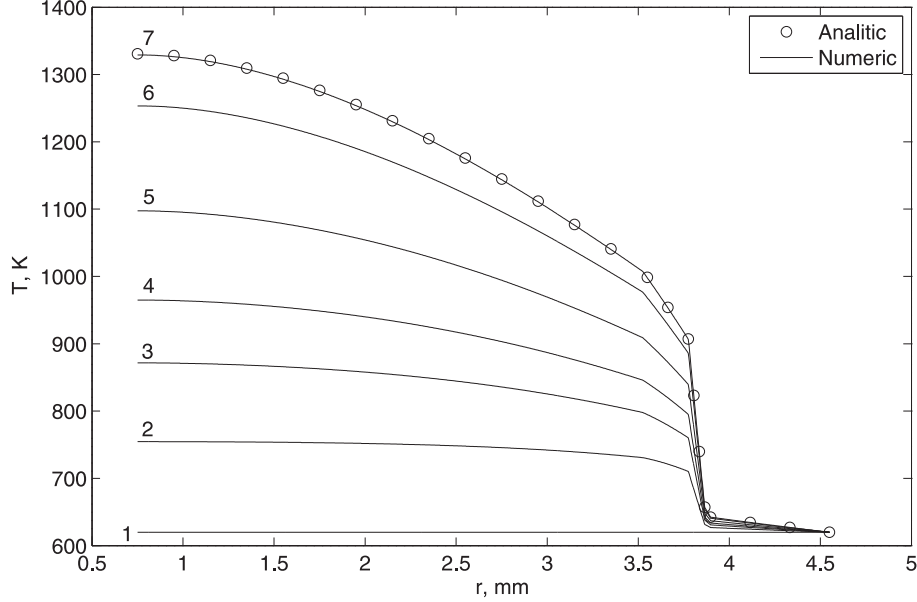


Figure 2: Evolution of temperature in nuclear fuel rod for high burn-up for  $q_L = 200 \text{ W/cm}$ . 1:  $t = 0 \text{ s}$ ; 2:  $t = 1 \text{ s}$ ; 3:  $t = 2 \text{ s}$ ; 4:  $t = 3 \text{ s}$ ; 5:  $t = 5 \text{ s}$ ; 6:  $t = 10 \text{ s}$ ; 7:  $t = 30 \text{ s}$ ;

#### 4 The statement of the stationary problem for the temperature distribution in nuclear fuel rods with the rim - layer and the zirconium oxide

Using the numerical simulation we have obtained in the previous section that the basic behavior of the nuclear fuel rod is stationary. Consequently we can consider the temperature distribution in the nuclear fuel rod taking the above mentioned problem when  $\frac{\partial T}{\partial t} = 0$ . In this case we have the following statement of the problem for the temperature distribution

$$\frac{1}{r} \frac{d}{dr} \left( \frac{r}{A + BT_1} \frac{dT_1}{dr} \right) + q = 0, \quad r_0 < r < \tilde{R}_0 \quad (23)$$

$$\frac{1}{r} \frac{d}{dr} \left( \frac{r}{A_1 + B_1 \tilde{T}_1} \frac{d\tilde{T}_1}{dr} \right) + q_1 = 0, \quad \tilde{R}_0 < r < R_0 \quad (24)$$

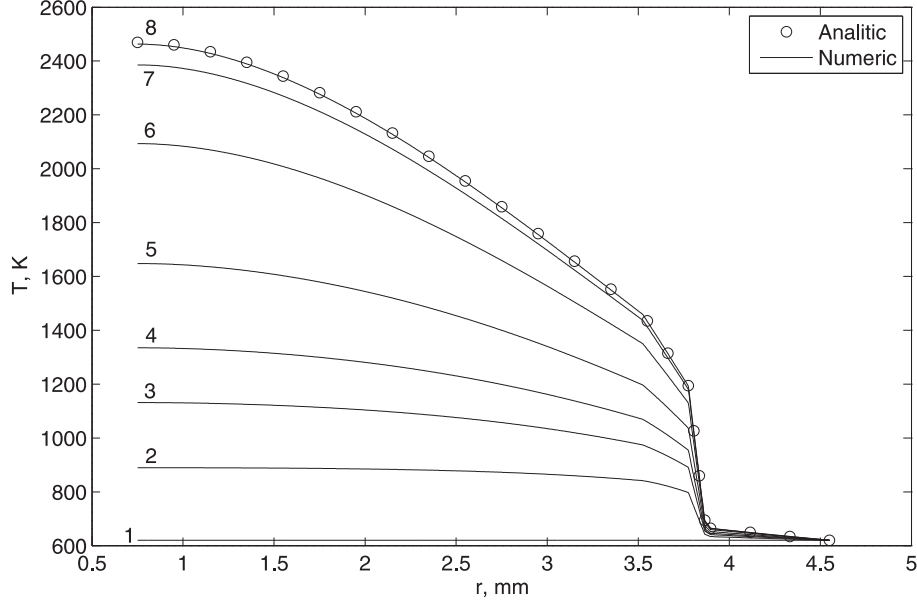


Figure 3: Evolution of temperature in the nuclear fuel rod for high burn-up at  $q_L = 400$  W/cm. 1:  $t = 0$  s; 2:  $t = 1$  s; 3:  $t = 2$  s; 4:  $t = 3$  s; 5:  $t = 5$  s; 6:  $t = 10$  s; 7:  $t = 20$  s; 8:  $t = 40$  s;

$$\frac{1}{r} \frac{d}{dr} \left( r \lambda_1 \frac{dT_2}{dr} \right) = 0, \quad R_0 < r < R_1 \quad (25)$$

$$\frac{1}{r} \frac{d}{dr} \left( r \tilde{\lambda}_2 \frac{d\tilde{T}_3}{dr} \right) = 0, \quad R_1 < r < \tilde{R}_2 \quad (26)$$

$$\frac{1}{r} \frac{d}{dr} \left( r \lambda_2 \frac{dT_3}{dr} \right) = 0, \quad \tilde{R}_2 < r < R_2 \quad (27)$$

where  $T_1(r)$  is the dependence of the temperature on radius in the fuel,  $\tilde{T}_1(r)$  is the dependence of the temperature on radius in the rim layer,  $T_2(r)$  is the dependence of the temperature on radius in the gap,  $\tilde{T}_3(r)$  is the dependence of the temperature on radius in the zirconium oxide,  $T_3(r)$  is the dependence of the temperature on radius in the cladding,  $q$  and  $q_1$  are volumetric sources in the fuel and in the rim - layer.

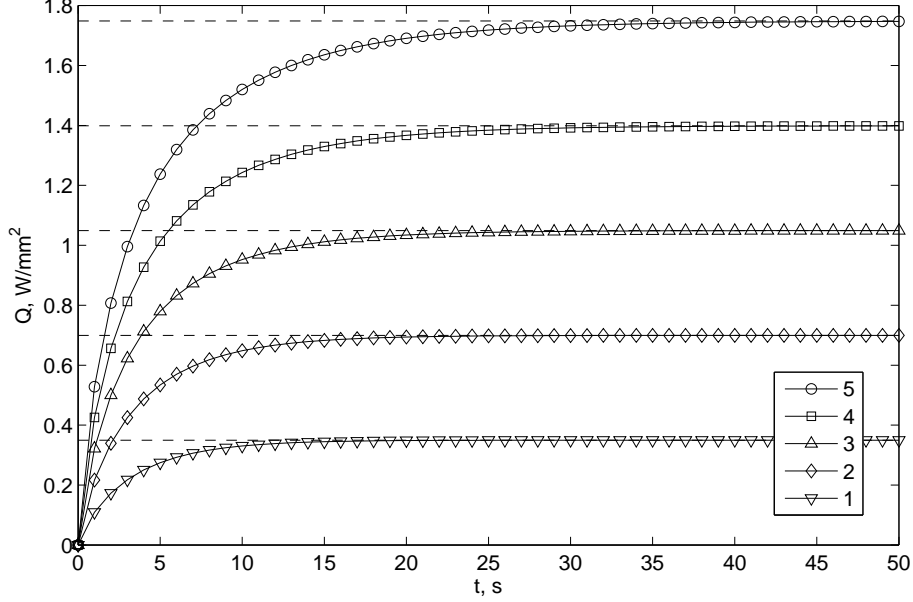


Figure 4: Dependence of the heat flow on time via surface at  $r = R_2$  for sources 1:  $q_L = 100$  W/cm; 2:  $q_L = 200$  W/cm; 3:  $q_L = 300$  W/cm; 4:  $q_L = 400$  W/cm; 5:  $q_L = 500$  W/cm; ( $bu = 120$ )

To obtain the solution of the system of equations (23) - (27) we have to add the boundary values for this system of equations. In this case we use the boundary conditions at  $r = r_0$ ,  $r = \tilde{R}_0$ ,  $r = R_0$ ,  $r = R_1$ ,  $r = \tilde{R}_2$  and at  $r = R_2$ .

The boundary value for the temperature  $T_1(r)$  at  $r = r_0$  takes the form

$$\left. \frac{dT_1}{dr} \right|_{r=r_0} = 0. \quad (28)$$

We have conditions at  $r = \tilde{R}_0$  in the form

$$\frac{1}{A + BT_1} \left. \frac{dT_1}{dr} \right|_{r=\tilde{R}_0} = \frac{1}{A_1 + B_1\tilde{T}_1} \left. \frac{d\tilde{T}_1}{dr} \right|_{r=\tilde{R}_0}, \quad (29)$$

$$T_1(r = \tilde{R}_0) = \tilde{T}_1(r = \tilde{R}_0).$$

In the case  $r = R_0$ , we use the following conditions

$$\frac{1}{A_1 + B_1\tilde{T}_1} \left. \frac{d\tilde{T}_1}{dr} \right|_{r=R_0} = \lambda_1 \left. \frac{dT_2}{dr} \right|_{r=R_0}, \quad \tilde{T}_1(r = R_0) = T_2(r = R_0). \quad (30)$$

We take the conditions at  $r = R_1$

$$\lambda_1 \left. \frac{dT_2}{dr} \right|_{r=R_1} = \tilde{\lambda}_2 \left. \frac{d\tilde{T}_3}{dr} \right|_{r=R_1}, \quad T_2(r = R_1) = \tilde{T}_3(r = R_1). \quad (31)$$

Assuming the flow at  $r = \tilde{R}_2$  we obtain the conditions

$$\tilde{\lambda}_2 \left. \frac{d\tilde{T}_3}{dr} \right|_{r=\tilde{R}_2} = \lambda_2 \left. \frac{dT_3}{dr} \right|_{r=\tilde{R}_2}, \quad \tilde{T}_3(r = \tilde{R}_2) = T_3(r = \tilde{R}_2). \quad (32)$$

We believe that temperature on the surface of the cladding at  $r = R_2$  is constant and this temperature is equals to the temperature on the wall  $T_w$  [6]

$$T_3(r = R_2) = T_w. \quad (33)$$

System of equations (23) - (27) and conditions (28) - (33) describe the stationary temperature in the nuclear fuel rod.

## 5 Exact solutions for the temperature distribution in the stationary nuclear fuel rod with rim - layer and film of zirconium oxide

Solutions of the system of equations (23) — (33) can be obtained in the analytical form. Integrating equation (23) with respect to  $r$ , we have

$$\frac{r}{A + B T_1} \frac{dT_1}{dr} + \frac{q r^2}{2} = C_1, \quad (34)$$

where  $C_1$  is arbitrary constant.

Eq.(34) can be written as

$$\frac{d \ln(A + B T_1)}{dr} + \frac{B q r}{2} = \frac{B C_1}{r}. \quad (35)$$

Integrating Eq.(35) with respect to  $r$  again we obtain

$$\ln(A + B T_1) = \ln(C_2) + B C_1 \ln(r) - \frac{B q r^2}{4}, \quad (36)$$

where  $C_2$  is arbitrary constant as well. From Eq.(36) we have the solution of Eq.(23)

$$T_1(r) = \frac{C_2}{B} r^{BC_1} e^{-\frac{Bqr^2}{4}} - \frac{A}{B}. \quad (37)$$

By analogue we find the solution of Eq. (24) for dependence temperature on radius in rim layer

$$\tilde{T}_1(r) = \frac{\tilde{C}_2}{B_1} r^{B_1\tilde{C}_1} e^{-\frac{B_1q_1r^2}{4}} - \frac{A_1}{B_1}, \quad (38)$$

where  $\tilde{C}_1$  and  $\tilde{C}_2$  are constants of integration as well.

The general solutions of Eqs. (25) - (27) are determined by formulae

$$T_2(r) = \frac{C_3}{\lambda_1} \ln(r) + C_4, \quad (39)$$

$$\tilde{T}_3(r) = \frac{\tilde{C}_5}{\tilde{\lambda}_2} \ln(r) + \tilde{C}_6, \quad (40)$$

$$T_3(r) = \frac{C_5}{\lambda_2} \ln(r) + C_6, \quad (41)$$

where  $C_3$ ,  $C_4$ ,  $\tilde{C}_5$ ,  $\tilde{C}_6$ ,  $C_5$ , and  $C_6$  are arbitrary constants as well.

In order to find the temperature distribution in the nuclear fuel rod we have to obtain values of the arbitrary constants  $C_1$ ,  $C_2$ ,  $\tilde{C}_1$ ,  $\tilde{C}_2$ ,  $C_3$ ,  $C_4$ ,  $\tilde{C}_5$ ,  $\tilde{C}_6$ ,  $C_5$ , and  $C_6$  taking conditions (28) - (33) into account.

Taking the boundary value into account

$$\left. \frac{dT_1}{dr} \right|_{r=r_0} = 0, \quad (42)$$

we obtain the constant  $C_1$  in the form

$$C_1 = \frac{qr_0^2}{2}. \quad (43)$$

Substituting solutions (37) - (41) into conditions (28) - (33), we have the system of algebraic equations with respect to constants  $C_2$ ,  $\tilde{C}_1$ ,  $\tilde{C}_2$ ,  $C_3$ ,  $C_4$ ,  $\tilde{C}_5$ ,  $\tilde{C}_6$ ,  $C_5$ ,  $C_6$ . This system of equations takes the form

$$\frac{C_2}{B} \tilde{R}_0^{\frac{qBr_0^2}{2}} e^{-\frac{Bq\tilde{R}_0^2}{4}} - \frac{A}{B} = \frac{\tilde{C}_2}{B_1} \tilde{R}_0^{B_1\tilde{C}_1} e^{-\frac{B_1q_1\tilde{R}_0^2}{4}} - \frac{A_1}{B_1}, \quad (44)$$

$$\frac{qr_0^2}{2\tilde{R}_0} - \frac{q\tilde{R}_0}{2} = \frac{\tilde{C}_1}{\tilde{R}_0} - \frac{q_1\tilde{R}_0}{2}, \quad (45)$$

$$\frac{\tilde{C}_2}{B_1} R_0^{B_1\tilde{C}_1} e^{-\frac{B_1q_1R_0^2}{4}} - \frac{A_1}{B_1} = \frac{C_3}{\lambda_1} \ln R_0 + C_4, \quad (46)$$

$$\frac{\tilde{C}_1}{R_0} - \frac{q_1R_0}{2} = \frac{C_3}{R_0}, \quad (47)$$

$$\frac{C_3}{\lambda_1} \ln R_1 + C_4 = \frac{\tilde{C}_5}{\lambda_2} \ln R_1 + \tilde{C}_6, \quad (48)$$

$$C_3 = \tilde{C}_5, \quad (49)$$

$$\frac{\tilde{C}_5}{\lambda_2} \ln \tilde{R}_2 + \tilde{C}_6 = \frac{C_5}{\lambda_2} \ln \tilde{R}_2 + C_6, \quad (50)$$

$$\tilde{C}_5 = C_5, \quad (51)$$

$$\frac{C_5}{\lambda_2} \ln R_2 + C_6 = T_w. \quad (52)$$

Solving this system of equations with respect to constants  $C_2, \tilde{C}_1, \tilde{C}_2, C_3, C_4, \tilde{C}_5, \tilde{C}_6, C_5, C_6$ , we obtain dependencies of them on parameters of task in the form

$$C_2 = B \left\{ T_w + \frac{A_1}{B_1} + \left( \frac{q(r_0^2 - \tilde{R}_0^2)}{2} + \frac{q_1(\tilde{R}_0^2 - R_0^2)}{2} \right) \ln \left[ \left( \frac{\tilde{R}_2}{R_1} \right)^{\frac{1}{\lambda_2}} \left( \frac{R_1}{R_2} \right)^{\frac{1}{\lambda_2}} \left( \frac{R_0}{R_1} \right)^{\frac{1}{\lambda_1}} \right] \right\} \cdot \left( \frac{\tilde{R}_0}{R_0} \right)^{\frac{B_1q(r_0^2 - \tilde{R}_0^2) + B_1q_1\tilde{R}_0^2}{2}} \tilde{R}_0^{-\frac{-qBr_0^2}{2}} e^{\frac{q_1B_1(R_0^2 - \tilde{R}_0^2) + qB\tilde{R}_0^2}{4}} + \left( A - \frac{A_1B}{B_1} \right) \tilde{R}_0^{-\frac{-qBr_0^2}{2}} e^{\frac{qB\tilde{R}_0^2}{4}},$$

(53)

$$\tilde{C}_1 = \frac{q(r_0^2 - \tilde{R}_0^2)}{2} + \frac{q_1(\tilde{R}_0^2)}{2}, \quad (54)$$

$$\tilde{C}_2 = \left\{ B_1 T_w + A_1 + B_1 C_3 \ln \left[ \left( \frac{\tilde{R}_2}{R_1} \right)^{\frac{1}{\lambda_2}} \left( \frac{R_1}{R_2} \right)^{\frac{1}{\lambda_2}} \left( \frac{R_0}{R_1} \right)^{\frac{1}{\lambda_1}} \right] \right\} R_0^{-B_1 \tilde{C}_1} e^{\frac{B_1 q_1 R_0^2}{4}}, \quad (55)$$

$$C_3 = \frac{q(r_0^2 - \tilde{R}_0^2)}{2} + \frac{q_1(\tilde{R}_0^2 - R_0^2)}{2}, \quad (56)$$

$$C_4 = T_w - \left( \frac{q(r_0^2 - \tilde{R}_0^2)}{2} + \frac{q_1(\tilde{R}_0^2 - R_0^2)}{2} \right) \ln \left[ \left( \frac{R_2}{\tilde{R}_2} \right)^{\frac{1}{\lambda_2}} \left( \frac{\tilde{R}_2}{R_1} \right)^{\frac{1}{\lambda_2}} R_1^{\frac{1}{\lambda_1}} \right], \quad (57)$$

$$\tilde{C}_5 = \frac{q(r_0^2 - \tilde{R}_0^2)}{2} + \frac{q_1(\tilde{R}_0^2 - R_0^2)}{2}, \quad (58)$$

$$\tilde{C}_6 = T_w - \left( \frac{q(r_0^2 - \tilde{R}_0^2)}{2} + \frac{q_1(\tilde{R}_0^2 - R_0^2)}{2} \right) \ln \left[ \left( \frac{R_2}{\tilde{R}_2} \right)^{\frac{1}{\lambda_2}} \left( \tilde{R}_2^{\frac{1}{\lambda_2}} \right) \right]. \quad (59)$$

$$C_5 = \frac{q(r_0^2 - \tilde{R}_0^2)}{2} + \frac{q_1(\tilde{R}_0^2 - R_0^2)}{2}, \quad (60)$$

$$C_6 = T_w - \left( \frac{q(r_0^2 - \tilde{R}_0^2)}{2} + \frac{q_1(\tilde{R}_0^2 - R_0^2)}{2} \right) \ln \left( R_2^{\frac{1}{\lambda_2}} \right). \quad (61)$$

Substituting these constants into the general solutions of the system of equations we have formulae to determine the temperature distribution in the nuclear fuel rod. The temperature distribution in the fuel without rim - layer takes the form

$$\begin{aligned}
T_1(r) = & \left\{ T_w + \frac{A_1}{B_1} + W_0 \ln \left[ \left( \frac{r}{R_1} \right)^{\frac{1}{\lambda_1}} \left( \frac{R_1}{\tilde{R}_2} \right)^{\frac{1}{\lambda_2}} \left( \frac{\tilde{R}_2}{R_2} \right)^{\frac{1}{\lambda_2}} \right] \right\} \\
& \cdot \left( \frac{\tilde{R}_0}{R_0} \right)^{B_1 W_1} \left( \frac{r}{\tilde{R}_0} \right)^{\frac{q B r_0^2}{2}} e^{\frac{q_1 B_1 (R_0^2 - \tilde{R}_0^2) + q B (\tilde{R}_0^2 - r^2)}{4}} + \\
& + \left( \frac{A}{B} - \frac{A_1}{B_1} \right) \left( \frac{r}{\tilde{R}_0} \right)^{\frac{q B r_0^2}{2}} e^{\frac{q B (\tilde{R}_0^2 - r^2)}{4}} - \frac{A}{B},
\end{aligned} \tag{62}$$

where we use the notation

$$W_0 = \frac{q (r_0^2 - \tilde{R}_0^2)}{2} + \frac{q_1 (\tilde{R}_0^2 - R_0^2)}{2}, \quad W_1 = \frac{q (r_0^2 - \tilde{R}_0^2)}{2} + \frac{q_1 \tilde{R}_0^2}{2}. \tag{63}$$

The temperature distribution in the rim - layer has dependence on parameters of task and on the radius in the form

$$\begin{aligned}
\tilde{T}_1(r) = & \left\{ T_w + \frac{A_1}{B_1} + W_0 \ln \left[ \left( \frac{r}{R_1} \right)^{\frac{1}{\lambda_1}} \left( \frac{R_1}{\tilde{R}_2} \right)^{\frac{1}{\lambda_2}} \left( \frac{\tilde{R}_2}{R_2} \right)^{\frac{1}{\lambda_2}} \right] \right\} \\
& \cdot \left( \frac{r}{R_0} \right)^{B_1 W_1} e^{\frac{q_1 B_1 (R_0^2 - r^2)}{4}} - \frac{A_1}{B_1}.
\end{aligned} \tag{64}$$

The temperature distribution in the gap can be written as

$$T_2(r) = T_w + W_0 \ln \left[ \left( \frac{r}{R_1} \right)^{\frac{1}{\lambda_1}} \left( \frac{R_1}{\tilde{R}_2} \right)^{\frac{1}{\lambda_2}} \left( \frac{\tilde{R}_2}{R_2} \right)^{\frac{1}{\lambda_2}} \right]. \tag{65}$$

The temperature in the film of the zirconium oxide is expressed by formula

$$\tilde{T}_3(r) = T_w + W_0 \ln \left[ \left( \frac{r}{\tilde{R}_2} \right)^{\frac{1}{\lambda_2}} \left( \frac{\tilde{R}_2}{R_2} \right)^{\frac{1}{\lambda_2}} \right]. \tag{66}$$

The temperature distribution in the cladding is found by formula

$$T_3(r) = T_w + W_0 \ln \left[ \left( \frac{r}{R_2} \right)^{\frac{1}{\lambda_2}} \right]. \tag{67}$$



The temperature distribution in the nuclear fuel rod is described by the continuous function with the break of the first derivative

$$T(r) = \begin{cases} T_1(r), & \text{if } r_0 \leq r < \tilde{R}_0, \\ \tilde{T}_1(r), & \text{if } \tilde{R}_0 \leq r < R_0, \\ T_2(r), & \text{if } R_0 \leq r < R_1, \\ \tilde{T}_3(r), & \text{if } R_1 \leq r < \tilde{R}_2, \\ T_3(r), & \text{if } \tilde{R}_2 \leq r < R_2. \end{cases} \quad (68)$$

Using formula (68) we can find the temperature distribution in the nuclear fuel rod at given volumetric source rate in the fuel  $q$  and in the rim - layer  $q_1$ . We can find the temperature distribution in the case of different thickness of the film for the zirconium oxide and at different sizes of the rim - layer. From formulae (62) - (67) we can obtain a number of partial dependencies for the temperature distribution in nuclear fuel rod. We can find the temperature distribution in the nuclear fuel rod without rim - layer, without the zirconium oxide, without gap and so on. With this aim we have to take  $\tilde{R}_0 = R_0$  (rim - layer is absent),  $\tilde{R}_2 = R_2$  (the zirconium oxide is absent),  $R_0 = R_1$  (gap is absent) and so on.

## 6 Results and discussion

Let us consider the temperature distribution in a nuclear fuel rod taking the rim - layer and the film of zirconium oxide into account. To analyze the temperature distribution we use sizes of nuclear fuel rod from the table 1.

Table 1: Parameters of the nuclear fuel element

$r_0$ , mm	$R_0$ , mm	$R_1$ , mm	$R_2$ , mm
0.75	3.775	3.865	4.550

Parameters of heat conductivities of the fuel, the helium in the gap, the film of the zirconium oxide and the cladding of the zirconium are given in the table 2. We assume, that the heat conductivity is 2 times less in a rim—layer, than the heat conductivity in the fuel core.

Table 2: Parameters of heat conductivities of fuel element

$A$ , mm·K/W	$B$ , mm/W	$\lambda_1$ , W/mm·K	$\tilde{\lambda}_2$ , W/mm·K	$\lambda_2$ , W/mm·K	$T_w$ , K
43.8	0.2294	$0.3 \cdot 10^{-3}$	$1.8 \cdot 10^{-3}$	$22.0 \cdot 10^{-3}$	620

We assume that the temperature of the coolant  $T_w$  is equal to 620 K ( $\simeq 350^\circ\text{C}$ ).

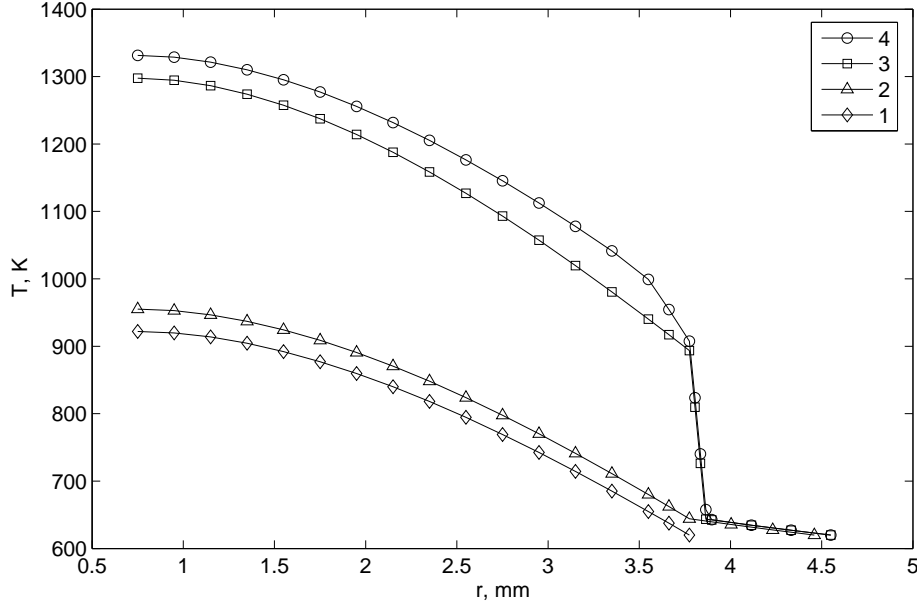


Figure 5: Dependence of temperature on radius at  $q_L = 200 \text{ W/cm}$  for cases: 1: gap and cladding are out; 2: gap is absent; 3:  $bu = 0$ ; 4:  $bu = 120$ ;

Some thermal regimes of temperature distributions in the nuclear fuel rod are given on figure 5 and on figure 6 by the formulae (62) — (67). The first figure illustrates curves for the value of the source  $q_L = 200 \text{ W/cm}$ . The second figure demonstrates the thermal regimes in the case of the source  $q_L = 400 \text{ W/cm}$ .

Curve 1 illustrates the temperature distribution when the gap and the cladding are absent. This case is possible when there is breakage of the cladding and the coolant has contact with the fuel. Temperature of the fuel in this case is less than in other cases. The decreasing of temperature derives from the fact that energy of the fuel goes to the coolant because the heat conductivity of fuel is more than the heat conductivity of the helium in the gap.

Curve 2 in figures corresponds to the case with cladding but when the gap is absent. One can observe that the temperature is higher than in previous case but this one is less than the temperature in the nuclear fuel rod for the normal behavior.

Curve 3 illustrates the case of the normal behavior of the nuclear fuel rod.

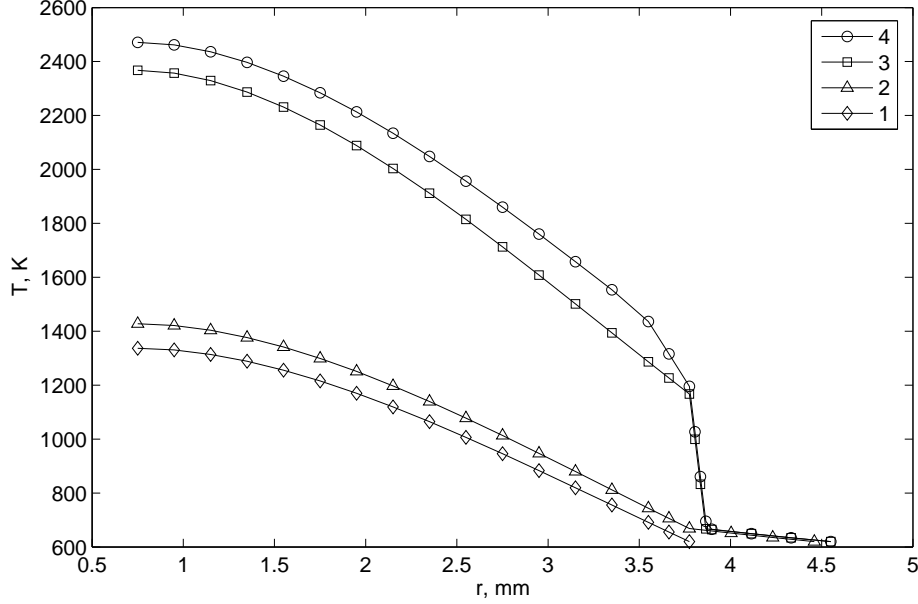


Figure 6: Dependence of temperature on radius at source  $q_L = 400$  W/cm for cases: 1: gap and cladding are absent; 2: gap is absent; 3:  $bu = 0$ ; 4:  $bu = 120$ ;

The temperature distribution is higher of the previous cases but this one is less then in the case with the formation of the rim - layer.

Curve 4 on figure 5 and on figure 6 corresponds to the thermal regime in nuclear fuel rod of high burn-up. We take into account the burn-up equal 120. We can see that the temperature in this case of the nuclear fuel rod is much more then other cases. The comparison of the temperature in this case with the point of the melting fuel shows that there is dangerous behavior of the nuclear reactor because it is possible the melting of the fuel at formation of the rim - layer. This fact illustrates that in the case of increasing of the rim - layer we have to decrease the value of the source.

At numerical calculations we suppose that the film of the zirconium oxide is formed at the expense of the gap and the cladding at various values of burn-up of the fuel. As this takes place the thickness of the gap is decreased. We assume that the film of the zirconium oxide takes 90 % of the cladding and 10 % of the volume in the gap.

The dependence of temperature on radius in the case of the normal behavior in nuclear fuel rod and for high burn-up is given in figure 7 ( $q = 0.2$ ) and in figure 8 ( $q=0.4$ ).

Table 3: Parameters at burn-up of fuel

Burn-up, GWt · twenty four hours/t·U	0	60	80	100	120
Thickness of a layer $ZrO_2$ , mm	0	0.0168	0.0224	0.028	0.0336
Thickness of a rim — layer, mm	0	0.1	0.15	0.2	0.25

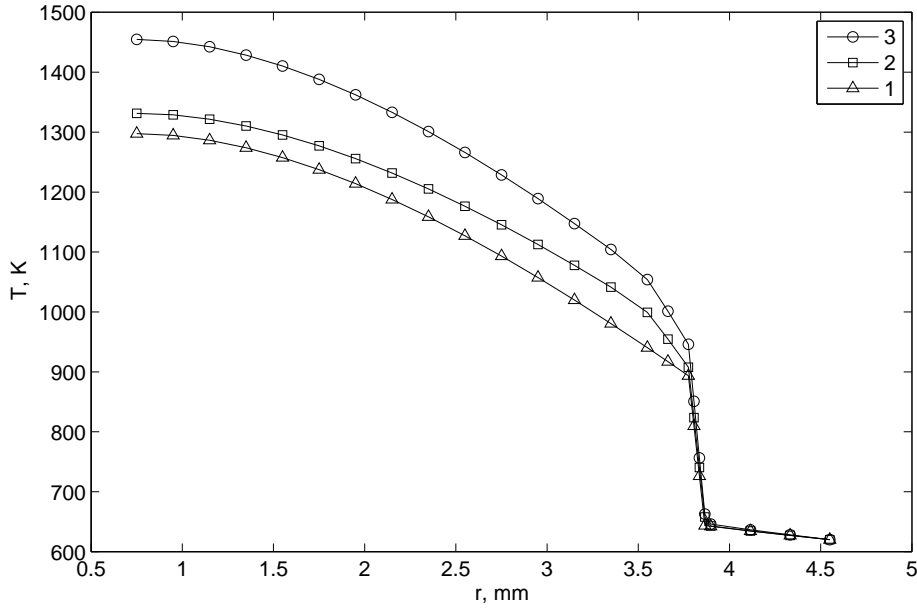


Figure 7: Dependence of temperature on radius at  $q_L = 200$  W/cm for cases: 1:  $bu = 0$ ; 2:  $bu = 120$  ( $q_L = 200$  W/cm); 3:  $bu = 120$  ( $q_L = 227$  W/cm)

We can observe that the high burn-up leads to the increasing of the temperature in nuclear fuel rod. The point of the melting of  $UO_2$  is equal to 3000 K. In the case of the high burn-up equal to 120 we can believe that the fuel can melt and we need to decrease the power of the source in the nuclear fuel rod.

Dependence of temperature on source  $q$  in the point  $r = r_0$  of the nuclear fuel rod is presented in figure 9 at various depths of burn-up of the fuel.

From this figure we can see how should we have to increase the power in nuclear fuel rod to have the normal behavior of the fuel element. The formation of the rim - layer leads to increasing of the heat conductivity. As this fact takes place the power of the source in nuclear fuel rod is decreased. The linear power of the nuclear fuel rod is decreased as well. Temperature in the fuel and in the rim - layer is decreased. We can see this process in

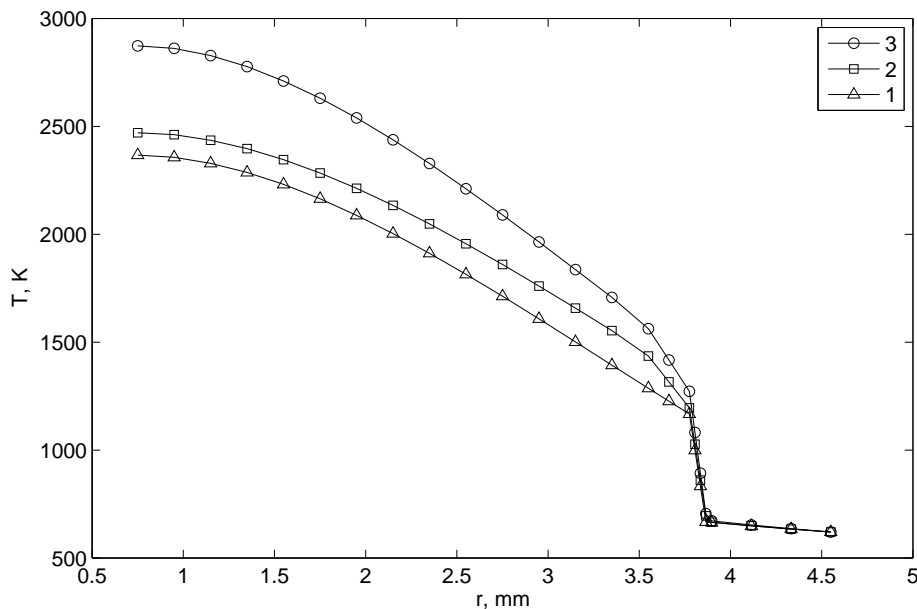


Figure 8: Dependence of temperature on radius at  $q = 300 \text{ W/cm}$  for cases: 1:  $bu = 0$ ; 2:  $bu = 120$  ( $q_L = 4 \text{ W/cm}$ ); 3:  $bu = 120$  ( $q_L = 453 \text{ W/cm}$ )

figure 7 and in figure 8. Therefore we have to increase the power in nuclear fuel rod.

## 7 Conclusion

Let us shortly formulate results of this paper. We have studied the temperature distribution in nuclear fuel rod taking into account the fuel, the rim - layer, the gap, the film of the zirconium oxide and the cladding. Solving the nonstationary task of the temperature distribution in the nuclear fuel rod by the numerical simulation we have obtained that the evolution of the temperature in the rod to the stationary behavior goes the short time. This time is less then 45 seconds for the maximum power in nuclear fuel rod. This fact allowed us to consider the solution of the stationary behavior of the nuclear reactor. We have solved this task using the analytical method and we have found the exact solution of the temperature distribution in the nuclear fuel rod. We analyzed the different thermal regimes for the stationary behavior reactor and have shown the important role of the rim - layer of high burn-up nuclear fuel rod.

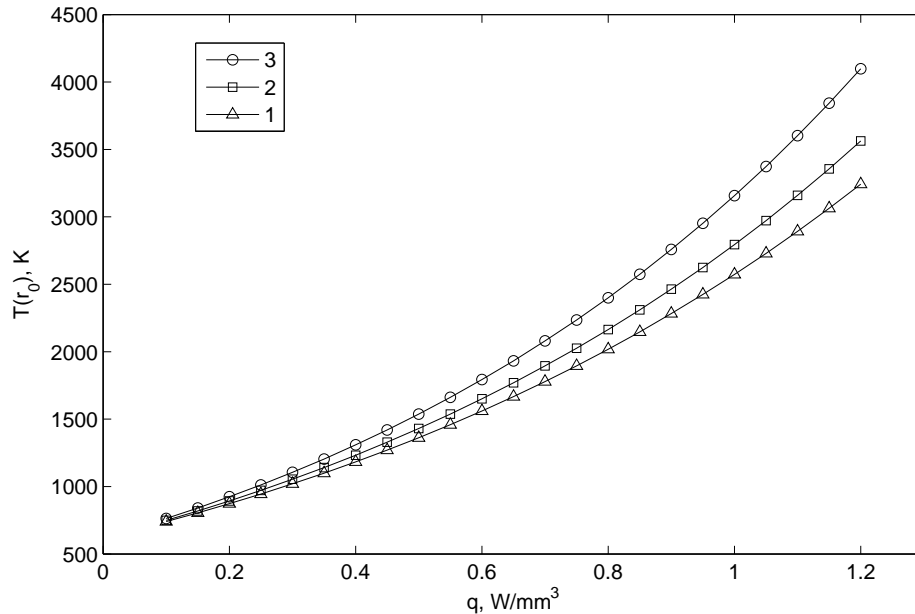


Figure 9: Dependence of temperature in point  $r = r_0$  on linear power of nuclear fuel rod ( $q_1 = 2q$ ) at different burn-up 1:  $bu = 0$ ; 2:  $bu = 60$ ; 3 :  $bu = 120$ ;

## References

- [1] Amaya, M., Une K., Minato K. Heat capacity measurements on unirradiated and irradiated fuel pellets// Journal of Nuclear Materials., 294 (2001), 1–7.
- [2] Yapici, H., Ipek, O., Ubeyli, M Investigation of the performance parameters and temperature distribution in fuel rod dependence on operation periods and first wall loads in fusion-fusion reactor system fueled with ThO<sub>2</sub>. Energy Convers Manage. 44, (2003), 573–595
- [3] Kim, H.T., Rhee, B.W., Park, J.J. Application of the finite volume method to the radial conduction model of the CATHENNA code. Ann. Nucl. Energy 33, (2006), 924–931
- [4] Pontedeiro Auro C., Cotta Renato M, Su Jian. Improved lumped model for thermal analysis of high burn-up nuclear fuel rods // Progress in Nuclear Energy. 50, (2008), 767–773.

- [5] Fortini Maria A., Stamoulis Michel N., Ferreira Angela F.M., Pereira Claudia, Costa Antonella L., Silva Clarysson Application of the orthogonal method to determination of temperature distribution in cylindrical conductors // *Annals of Nuclear Energy*. 35 (2008), 1681–1683.
- [6] Espinosa-Paredes, G., Nuñez-Carrera A., Vazquez-Rodriguez A. Simplified distributed parameters BWR dynamic model for transient and stability analysis. *Ann. Nucl. Energy* 33. (2006) 1245-1259
- [7] Espinosa-Paredes, G., Espinosa-Martinez, E-G. Fuel rod model based on Non-Fourier heat conduction equation. *Ann. Nucl. Energy*, 36 (2009) 680-693
- [8] Matzke, Hj. On the rim effect in high burnup UO<sub>2</sub> LWR fuels, *J. Nucl. Mater.* 189 (1992) 141-148.
- [9] Walker C.T. , Kameyama T., Kitajima, S., Kinoshita M. Concerning the microstructure changes that occur at the surface of UO<sub>2</sub> pellets on irradiation to high burnup, *J. Nucl. Mater.*, 188 (1992) 73.
- [10] Une, K. Nogita, K., Kashibe, S., Imanura, M. Microstructural change and its influence on fission gas release in high burnup UO<sub>2</sub> fuel, *J. Nucl. Mater.*, 188 (1992) 65.
- [11] Lassmann K., Walker C.T., Van de Laar J., Lindstrom F. Modelling the high burnup UO<sub>2</sub> structure in LWR fuel// *Journal of Nuclear Materials*, 1995. V. 226. P. 1-8.
- [12] Spino J., Vennix K. Coquerelee M. Detailed characterization of the rim microstructure in PWR fuels in the burn-up range 40-67 GWd/tM// *J. Nucl. Mater.*, 1996. V.231. P. 179-190.
- [13] Matzke Hj., Spino J. Formation of the rim structure in high burnup fuel// *J.Nucl.Mater.*, 1997. V. 248. . 170-179.
- [14] Kinoshita M. Towards the mathematical model of rim structure formation, *J. Nucl. Mater.* 248 (1997) 185-190.
- [15] Kinoshita M., Kameyama T., Kitajima S., and Matzke Hj. Temperature and fission rate effects on the rim structure formation in a UO<sub>2</sub> fuel with a burnup of 7.8
- [16] Walker C.T. Assessment of the radial extent and completion of recrystallisation in high burn-up UO<sub>2</sub> nuclear fuel by EPMA// *J. Nucl. Mater.*, 1999, V. 275. P. 56-62.

- [17] Romano A. et al. Evolution of porosity in the high-burnup fuel structure. *Journal of Nuclear Materials*, 2007. v. 361. P. 62-68.
- [18] Lee Byung-Ho, Koo Yang-Hyun and Sohn Dong-Seong. Rim Characteristics and Their Effects on the Thermal Conductivity in High Burnup  $UO_2$  Fuel, *Journal of Nuclear Science and Technology*. 38 (2001), 45–52
- [19] Kashibe, S., Une, K., Nogita, K., Formation and growth of intragranular fission gas bubbles in  $UO_2$  fuels with burn-up of 6 - 83 GWd/t, *J. Nucl. Mat.* 226 (1993) 22
- [20] Nogita, K. and Une, K. Irradiation-induced recrystallization in high burnup  $UO_2$  fuel, *J. Nucl. Mater.* 226 (1995), 302–310
- [21] *Kudryashov N.A., Loguinova N.B.* Be careful with Exp — function method, *Commun Nonlinear Sci Numer Simulat*, 14 (2009), 1881 –1890
- [22] *Kudryashov N.A.* On "new travelling wave solutions" of the KdV and the KdV — Burgers equations, *Commun Nonlinear Sci Numer Simulat* 14 (2009), 1891 –1900
- [23] *Kudryashov N.A.* Seven common errors in finding exact solutions of nonlinear differential equations, *Commun Nonlinear Sci Numer Simulat* 14 (2009), 2507 –2529
- [24] Minato, K., Shiratori, T., Serizawa, H., Hayashi, K., Une, K., Nogita, K., Hirai, M., Amaya, M., Thermal conductivities of irradiated  $UO_2$  and  $(U, Gd)O_2$ , *Journal of Nuclear Materials.*, 288 (2001) 57 - 65
- [25] Ronchi, C., Sheindlin, M., Staicu, D., Kinoshita, M., Effect of burn-up on the thermal conductivity of uranium dioxide up to 100.000 MWd/t, *Journal of Nuclear Materials.*, 327 (2004) 58 -76
- [26] El—Koliel, M.S., Abou—Zaid, A.A., El—Kafas A.A., Modeling of WWER-440 fuel pin behavior at extended burn-up, *Nuclear Engineering and Design*, 229 (2004) 113 -119
- [27] Morimoto, K., Kato, M., Ogasawara, M., Kashimura, M., Thermal conductivities of hypostoichiometric  $(U, P, Am)O_{2-x}$  oxide, *Journal of Nuclear Materials.*, 374 (2008) 378 - 385